# Aptamer targeting of the elongation factor 1A impairs hepatocarcinoma cells viability and potentiates bortezomib and idarubicin effects

Bruna Scaggiante[a,1], Rosella Farra[b,1], Barbara Dapas[a], Gabriele Baj[a], Gabriele Pozzato[c], Mario Grassi[b], Fabrizio Zanconati[c], Gabriele Grassi[a,*]

[a] Department of Life Sciences, University of Trieste, Italy
[b] Department of Industrial Engineering and Information Technology, University of Trieste, Italy
[c] Department of Medical, Surgery and Health Sciences, University of Trieste, Cattinara Hospital, Italy

ARTICLE INFO

Accepted 13 April 2016

*Keywords:*
Liposome-delivery
Cholesterol-delivery
Aptamer
eEF1A
HCC

ABSTRACT

The high morbidity and mortality of hepatocellular carcinoma (HCC) is mostly due to the limited efficacy of the available therapeutic approaches. Here we explore the anti-HCC potential of an aptamer targeting the elongation factor 1A (eEF1A), a protein implicated in the promotion of HCC. As delivery methods, we have compared the effectiveness of cationic liposome and cholesterol-mediated approaches.

A75 nucleotide long aptamer containing GT repetition (GT75) was tested in three HCC cell lines, HepG2, HuH7 and JHH6. When delivered by liposomes, GT75 was able to effectively reducing HCC cells viability in a dose and time dependent fashion. Particular sensitive were JHH6 where increased apoptosis with no effects on cell cycle were observed. GT75 effect was likely due to the interference with eEF1A activity as neither the mRNA nor the protein levels were significantly affected. Notably, cholesterol-mediated delivery of GT75 abrogated its efficacy due to cellular mis-localization as proven by fluorescence and confocal microscopic analysis. Finally, liposome-mediated delivery of GT75 improved the therapeutic index of the anticancer drugs bortezomib and idarubicin.

In conclusion, liposome but not cholesterol-mediated delivery of GT75 resulted in an effective delivery of GT75, causing the impairment of the vitality of a panel of HCC derived cells.

## 1. Introduction

Hepatocellular carcinoma (HCC) has a worldwide diffusion and it is characterized by high morbidity and mortality, mainly because the disease is often diagnosed at a late stage (Ferlay et al., 2015; Jemal et al., 2011). Moreover, available therapeutic approaches have limited efficacy and systemic chemotherapy is poorly effective due to the general HCC resistance to anticancer agents (Azmi et al., 2015). Thus, the development of novel therapeutic approaches and delivery systems for HCC are urgently necessary (Scaggiante et al., 2014b).

Among the novel drugs with potential therapeutic value for HCC, nucleic acid based drugs (NABDs) are emerging as very attractive molecules (Grassi et al., 2013; Scaggiante et al., 2011, 2013a). Particularly interesting are aptamers, short single-stranded sequences of DNA or RNA able to bind a specific target with high affinity. Aptamers can fold into several secondary and tertiary different structural elements that eventually confer the ability to bind the target molecule in a fashion different from the Watson-Crick base pairing. Aptamers have many advantages compared to antibodies as they are smaller, easier to select, can be directed against any target, are cheaper to produce, are more stable and are not immunogenic (Scaggiante et al., 2013a).

As delivery tools for our aptamer, we concentrated on cationic lipids and cholesterol. Cationic lipids (Burnett et al., 2011; Kanasty et al., 2013; Li and Szoka, 2007; Oh and Park, 2009; Whitehead et al., 2009; Wu and McMillan, 2009; Yin et al., 2014; Zhou et al., 2013) have been frequently used as NABD delivery systems. This is

* Corresponding author at: Department of Life Sciences, University Hospital of Cattinara, Strada di Fiume 447, 34134 Trieste, Italy.
*E-mail address:* ggrassi@units.it (G. Grassi).
[1] First co-authorship.

mostly due to their ability to form complexes with NABD, to protect them against degradation in the biological environment and to promote their cellular internalization (Barba et al., 2015; Bochicchio et al., 2015). Moreover, our previous experience (Farra et al., 2011) demonstrated that cationic lipids have the ability to deliver NABD homogeneously within the hepatic cells showing the tendency of a nuclear accumulation. This is a desirable feature for our study as eEF1A, the target chosen in this work (see below), mostly localize in the nuclear/cytoskeleton compartment. As an alternative option, we have considered the cholesterol-mediated delivery. Cholesterol was chosen because it can increase the uptake of oligonucleotides by cells equipped with cholesterol receptor, as it is the case of liver cells, thus conferring a certain degree of targeting specificity. Moreover, cholesterol is known to improve the oligonucleotide pharmacokinetic properties (Healy et al., 2004; Krutzfeldt et al., 2005; Manoharan, 2002), a useful feature for future studies in animal models. Finally, cholesterol-conjugated NABD form particles in the nano-size range that can be embedded into micro-size carriers amenable for arterial delivery to the tumor mass *in vivo* (Piscaglia and Bolondi, 2010).

The target of our aptamer is the eukaryotic elongation factor 1A (eEF1A), a protein involved in the elongation step of protein synthesis (Scaggiante et al., 2014a). The major isoforms of eEF1A proteins consist of the ubiquitous eEF1A1 and the tissue-specialized eEF1A2, whose expression is mostly confined to skeletal muscle, heart and nervous system. Beside the role in translation, considered the "canonical function" of eEF1As, both isoforms possess "non-canonical functions" essential for cellular homeostasis such as the involvement in the nuclear protein export (Mickleburgh et al., 2006), the regulation of RNAs stability (Yan et al., 2008), and the regulation of cell cycle and apoptosis (Lamberti et al., 2004). Both eEF1A proteins play a role in solid and hematologic human tumors, mainly due to the dysregulation of their non-canonical functions (Abbas et al., 2015) as described for many human tumors including HCC (Scaggiante et al., 2014a). We have observed that in human HCC cell lines, eEF1A1 and eEF1A2 are overexpressed and that this overexpression relates with cancer cell growth and differentiation phenotype (Grassi et al., 2007a). Moreover, eEF1A2 overexpression was detected in about half of HCC human tumor specimens suggesting a role in HCC etiology (Schlaeger et al., 2008a).

In this work, we explore the effects of eEF1A targeting by a single stranded DNA aptamer containing GT repetitions in HCC cell lines. We have previously demonstrated that GT aptamers containing either 27 (GT27) or 51 GT (GT51) repetitions can specifically bind to the eEF1A protein derived from the nuclear/cytoskeletal-enriched compartment of a variety of leukemic cells (Dapas et al., 2003a; Morassutti et al., 1999; Scaggiante et al., 2006a, 2013b, 1998). Notably, eEF1A targeting resulted in a remarkable impairment of cell vitality showing a potent antitumor effect in leukemic cells. Here, we investigate the effectiveness of a novel aptamer targeting eEF1A containing 75 GT repetitions (GT75). A longer aptamer is used as we observed (unpublished results) that in cell lines derived solid tumors, longer GT aptamers have an improved effectiveness compared to shorter ones. In addition, we explore the ability of GT75 to improve the therapeutic index of clinically used anticancer drugs. It has been suggested that the combination of different drugs can ameliorate the outcome of HCC patients (Cabibbo et al., 2012; Di Costanzo and Tortora, 2015). As clinically employed anticancer drugs, we have considered bortezomib and idarubicin. Bortezomib, a proteasome inhibitor indicated for the treatment of multiple myeloma and cell lymphoma, is also potentially active in inhibiting HCC cell growth (Baiz et al., 2014; Chen et al., 2015). Idarubicin, an inhibitor of topoisomerase II, is under evaluation as a locally delivered anti HCC drug (transarterial chemoembolization (Favelier et al., 2013)).

## 2. Materials and methods

### 2.1. UV crosslinking

In a final volume of 20 μl, 3 μg of total nuclear extract were incubated in 20 mM Hepes pH 7.9, 420 mM NaCl, 1.5 mM $MgCl_2$, 0.2 mM EDTA, 25% glycerol containing proteases and phosphatases inhibitors, 2 ng GT75 or GT27 labelled by (γ-32P)ATP and different fold molar excess of non-labelled GT27/CT27/GT75/CT75 and poli (dI-dC), as competitors. After 25 min incubation at room temperature, the samples were irradiated for 10 min at 302 nm utilizing a trans illuminator UV (BioRad Laboratorie). Then, 3 μl Laemmli sample buffer were added and the mixture was boiled for 5 min. The denatured samples were then loaded and resolved on a SDS-polyacrylamide gel.

### 2.2. Cell cultures

The human HCC derived cell lines HepG2, HuH7 and JHH6 were cultured as described (Farra et al., 2010, 2011) and assigned to high, medium and low hepatic differentiation grade on the base of the capacity to synthesize albumin and ferritin (Grassi et al., 2007b), known markers of hepatic differentiation.

### 2.3. Aptamer transfection and uptake studies

The sequence of the specific anti eEF1A aptamer GT-75 (Eurofins MWG Operon, Ebersberg, Germany) was: TGTTTGTTTGTTTGTTTGTTTGTTTGTTTGTTTGTTTGTTTGTTTGTTTGTTTGTTTGTTTGT; the sequence of the control aptamer CT-75 was: TCTTTCTTTCTTTCTTTCTTTCTTTCTTTCTTTCTTTCTTTCTTTCTTTCTTTCTTTCTTTCTTTCTTTCTTTCTTTCTTTCTTTCT.

The day before transfection, $3 \times 10^4$ HCC cells were seeded at a density of $6 \times 10^3$ cells/cm$^2$ in six well microplate in the presence of 3 ml of 10% fetal calf serum-containing medium. Transfections were performed either using the GT75 aptamer labelled at the 5′ end by FITC (uptake studies), or the unlabeled GT75 and the CT75 control aptamer (functional studies). Optimal transfection conditions were obtained by using Lipofectamine 2000 (1 mg/ml) at a weight ratio aptamer-transfectant of 1:3, 1:1 and 1:1 for HepG2, HuH7 and JHH6, respectively. At the aptamer-transfectant ratios of 1:3, 1:1 and 1:0.5, Lipofectamine 2000 was able to bind and thus retard the run of the aptamer of 90, 60 and 30% respectively, compared to the naked aptamer (Supl. mat 1).

The mixture Lipofectamine-aptamer was then administered to the cells for 4 h at 37 °C in the presence of serum-free medium. Afterwards, transfection medium was removed, cells were washed with 3 ml of PBS, trypsinized, re-suspended in 500 μl of PBS and the number of fluorescein-positive cell evaluated by flow cytometry (FACScanto, Becton Dickinson, DIVA software).

GT75 and CT75 cholesterol conjugated molecules (Eurogentec, Liege, Belgium) carried the cholesterol moiety on the 3′ end. For uptake studies, the GT75 aptamer, double conjugated with cholesterol (3′ end) and FITC (5′ end) and either non-complexed or complexed with Lipofectamine, was administered to JHH6, seeded on glass cover-slips 24 h in advance. After 4 h transfection, the medium was removed, the cells were washed with phosphate buffer saline solution (PBS) and fixed with 4% paraformaldehyde in PBS for 30 min at RT and then washed again for three times with PBS. Coverslips were mounted on microscope slides with a medium containing the DAPI stain (Vector Laboratories Inc., Burlingame, CA, USA). Cells were then incubated for 30 min at 37 °C protected from light.

For confocal microscopic analysis, following transfection, the membrane and the cytosckeleton of cells in suspension were stained by the vital dye FastDil™ (Molecular Probes, Eugene, OR,

USA) according to manufacturer instructions. All images were acquired using a Nikon C1si confocal microscope, equipped with a 488 nm argon laser and 561 nm diode laser. Light was delivered to the sample with an 80/20 reflector. The system was operated with a pinhole size of one Airy disk (30 μm). Electronic zoom was kept at minimum values for measurements to reduce potential bleaching. 60X Plan Apo objective was used, collecting series of optical images at 0.15 μm z resolution step size. Images were processed for z-projection by using ImageJ 1.44 m (NIH, Bethesda, USA). The staining quantification was performed and analyzed by the ImageJ tool ROI manager. Quantitative data were collected on all optical slices describing the selected subcellular structure and normalized for the relative area stack by stack. Quantitative analysis refers to at least three different experiments in which about 100 measures per condition were made.

### 2.4. Cell necrosis, viability and cell cycle analysis

Cell viability, evaluated by MTT test, was performed as described (Baiz et al., 2009) seeding $1.5 \times 10^3$, $2.5 \times 10^3$ and $1 \times 10^3$ cells of HepG2, HuH7, JHH6, respectively, in 96 microplate. In JHH6, cell necrosis was evaluated by lactate dehydrogenase (LDH) assay kit according to manufacturer instructions (BioVision Prod., Mountain View CA) as described (Baiz et al., 2009); apoptosis was performed as described (Baiz et al., 2009; Dapas et al., 2009). For cell cycle analysis, $3 \times 10^4$ JHH6 cells were cultured in 6 well plates and pulsed with bromodeoxyuridine (BrdU, 10 μM) 12 h before harvesting as described (Grassi et al., 2005) except that resuspension in ice cold 70% ethanol was protracted overnight, the treatment with 1 M HCl 0.5% BSA was prolonged to 1 h and incubation with fluorescein-isothiocyanate (FITC)-conjugated mouse monoclonal antibody (BD PharMigen) anti BrdU was

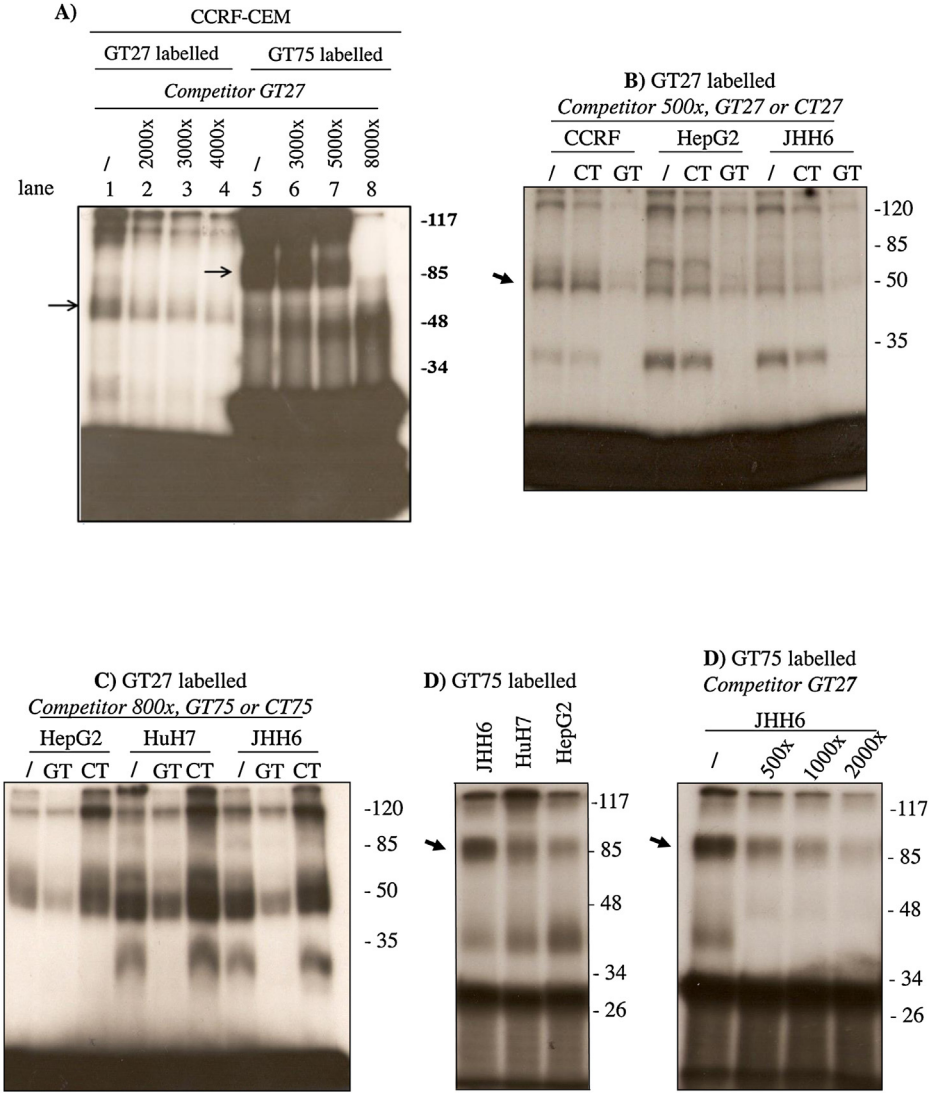


**Fig. 1.** GT27 and GT75 UV crosslinking assay. (A) $P^{32}$ labelled GT27 was mixed with total protein nuclear extracts of CCRF-CEM in the absence (lane 1) or presence (lanes 2–4) of increasing amount of non-labelled GT27; similarly, $P^{32}$ labelled GT75 was mixed with total protein nuclear extracts of CCRF-CEM in the absence (lane 5) or presence (lanes 6–8) of increasing amount of non-labelled d GT27. The arrows indicate the formation of the complexes of the expected sizes. (B) $P^{32}$ labelled GT27 was mixed with total protein nuclear extracts of CCRF-CEM, HepG2 and JHH6 alone (/) and in the presence of either non-labelled GT27 or the control non-labelled CT27; in all cases, complexes of the expected sizes were observed (arrow); additionally, non-labelled GT27 but not non-labelled CT27 displaced the complexes. (C) $P^{32}$ labelled GT27 was mixed with total protein nuclear extracts of HepG2, HuH7 and JHH6 alone (/) and in the presence of either non-labelled GT75 or the control non-labelled CT75; for all cell lines, complexes of the expected sizes were observed (arrow); additionally, non-labelled GT75 but not non-labelled CT75 displaced the complexes. (D) $P^{32}$ labelled GT75 was mixed with total protein nuclear extracts of HepG2, HuH7 and JHH6; complexes of the expected sizes (arrow) were visualized in all cases. (D) $P^{32}$ labelled GT75 was mixed with total protein nuclear extract of JHH6 alone (/) or in the presence of increasing amounts of cold GT75; non-labelled GT75 was able to displace the complexes (arrow) in a dose-dependent manner.

extended to 1 h. Finally, propidium Iodide (Sigma) and RNAsi (Sigma) were added one hour before flow-cytometry.

### 2.5. QRT-PCR

Total RNA was extracted, quantified and the quality evaluated as reported (Farra et al., 2011). Reverse transcription was performed using 500 ng of total RNA in the presence of random hexamers and MuLV reverse transcriptase (Applera Corporation, USA). The primers (MWG Biotech, GA, 300 nM) and the Real-Time amplification conditions for eEF1A were as described (Scaggiante et al., 2012). The relative amounts of the target mRNA were normalized by 28S rRNA content.

### 2.6. Western blotting

Protein extraction was performed as described (Scaggiante et al., 2012). Briefly, thirty μg of protein extract were resolved onto 12% SDS-PAGE and blotted onto a 0.22 μm nitrocellulose membrane (Schleicher & Schuell, Keene, NH). The rabbit monoclonal

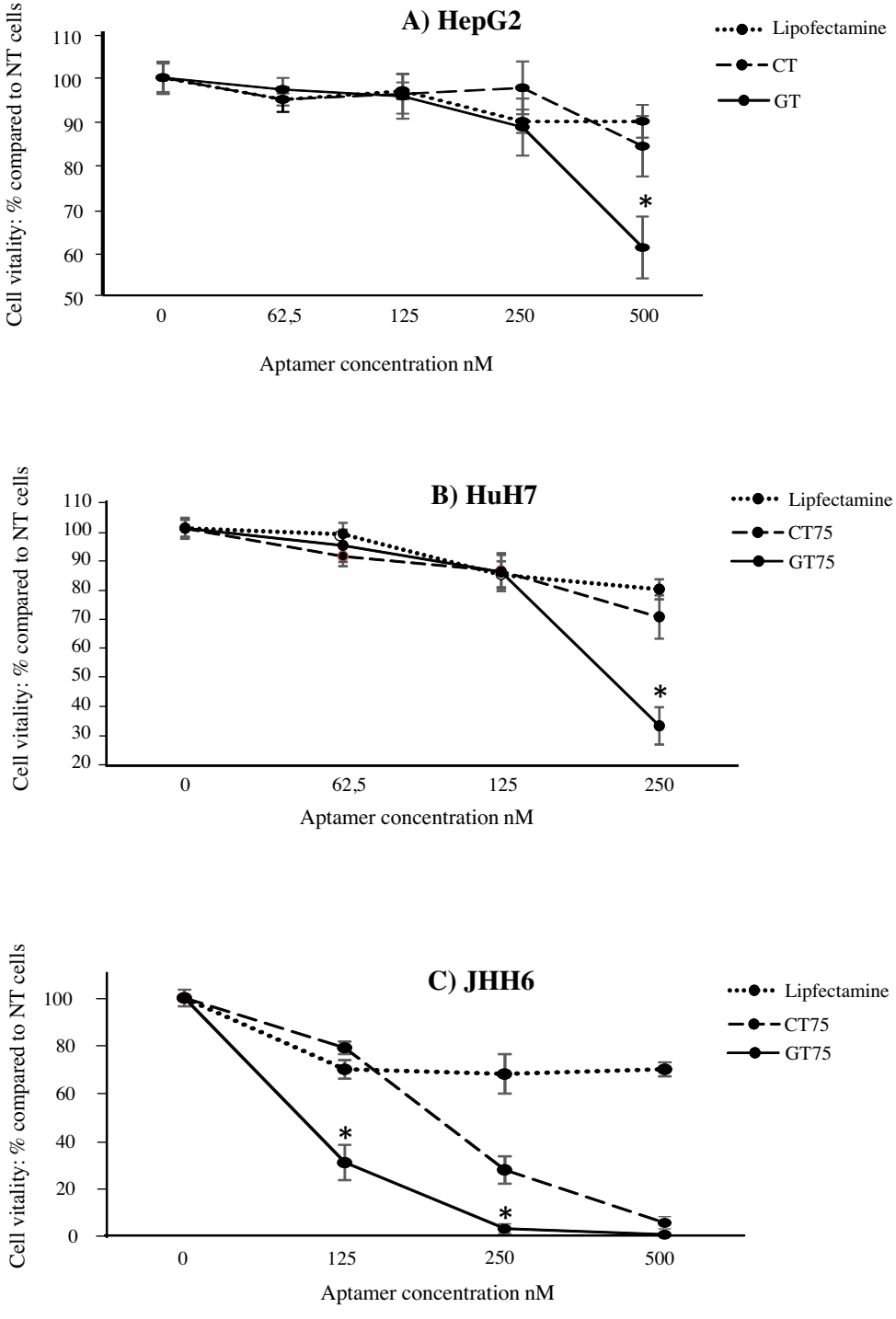


**Fig. 2.** Effects of GT75 on cell viability. Increasing amounts of GT75 and of the control CT75 were delivered by lipofection to 96-well-plate cultured HCC cells; the effects on cell viability were evaluated by MTT test 10 days after aptamer delivery. The results are reported as% of non-treated cells (NT); data are expressed as means ± SEM, n = 8. *$p < 0.004$, compared to NT.

antibody anti-eEF1A1 (AbCam, Cambridge, UK) and the rabbit polyclonal antibody anti-eEF1A2 (Santa Cruz, CA, USA) were used. In the same membrane, the loaded control protein GAPDH (Santa Cruz) was probed. Blots were developed using the corresponding secondary horseradish peroxidase antibodies (Santa Cruz, CA, USA) by enhanced chemiluminescence detection system (Pierce, Rockford, IL, USA) and exposed to Kodak film (Sigma-Aldrich, St. Louis, MO, USA).

### 2.7. Circular dichroism

Oligonucleotides were resuspended in buffer 150 mM NaCl, 10 mM $K_2HPO_4/KH_2PO_4$, 1 mM EDTA, pH 7.0 at concentration of 10 μm. After denaturation at 100 °C and renaturation overnight, the samples were diluted in 2 ml of buffer at the final concentration of 0.5 μM. The spectra from 220 to 320 nm wavelength were recorded by Jasco JT-710 equipped with software Spectra Manager™.

### 2.8. Combined aptamer/anti-cancer drug experiments

BZB (Velcade®, Janssen-Cilag International N.V., 0.09 mg Bortezomib/1 mg Velcade, w/w), was resuspended in phosphate buffer saline solution (PBS) and used at the indicated concentrations. Idarubicine (idarubicin hydrochloride, Pfizer, NY, USA) was resuspended in physiologic solution. For protocol 1, the drug was administered at day one after cell seeding followed the day after (two days after cell seeding) by aptamer transfection; MTT was then evaluated at day ten after cell seeding. For protocol 2, aptamer transfection was performed at day one after cell seeding followed by drug administration at day three after cell seeding; MTT was then evaluated at day ten after cell seeding.

### 2.9. Statistical analysis

P values were calculated by the GraphPad InStat tools (GraphPad Software, Inc., La Jolla, CA, USA) using the unpaired *t*-test with or without Welch correction and the Mann-Whitney Test, as appropriate. P values $< 0.05$ were considered statistically significant.

## 3. Results

### 3.1. GT75 aptamer binds to eEF1A as aptamer GT27

To demonstrate that the novel GT75 aptamer can bind the same target of GT27, *i.e.* eEF1A, UV-crosslinking were performed mixing labelled aptamers and proteins derived from total nuclear/cytoskeleton-enriched extracts. In T-lymphoblastic CCRF-CEM cells (Fig. 1A), previously employed to study GT27 effects (Scaggiante et al., 2006a, 2005, 1998), we confirm the formation of the expected 50 kDa complex using the GT27 labelled aptamer (Fig. 1A lane 1). Using the GT75 labelled aptamer, a complex near to 85 kDa was detected (Fig. 1A lane 5). This molecular weight (MW) is compatible with the combination of the MW of eEF1A protein and of the 75 long aptamer GT75. Importantly, the GT27-50 kDa and the GT75-85 kDa bands were efficiently displaced by a molar excess of the non-labelled GT27 (Fig. 1A lanes 2–4 and 6–8, respectively). This supports the conclusion that in CCRF-CEM cells, GT75 targets eEF1A as GT27 does.

We then tested in the HCC cell lines here considered, *i.e.* HepG2, HuH7 and JHH6, the ability of GT27 and GT75 to bind eEF1A. By using a labelled GT27, in the HCC cell lines HepG2 and JHH6 we observed the same complex as in CCRF-CEM (Fig. 1B). Comparable results were observed in the third HCC cell line here considered, *i.e.* HuH7 (data not shown). Notably, a molar excess of non-labelled GT27 but not of the control CT27 (unspecific aptamer containing CT repetition) displaced the complex. Moreover (Fig. 1C), the same occurred also in the presence of a molar excess of non-labelled GT75 but not of the non-labelled control CT75 (unspecific aptamer containing CT repetition). Finally, by using a labelled GT75, it was possible to obtain in the HCC cell lines considered, a complex comparable in weight to that observed in CCRF-CEM (compare Fig. 1A lane 5 with Fig. 1D). Importantly, in JHH6 the complex was displaced by a molar excess of non-labelled GT27. Comparable results were obtained for the other two HCC cell lines HepG2 and HuH7 (data not shown). Together, these observations support the concept of a specific GT75 binding to eFF1A in the HCC cell lines considered.

### 3.2. GT75 aptamer impairs the vitality of HCC cells

As models of HCC, we have considered HepG2, HuH7 and JHH6 as these cell lines display different phenotypes and thus phenotypic-related effects of eEF1A targeting by our aptamer can be studied. In particular, HepG2, HuH7 and JHH6 can be assigned to high medium and low hepatic differentiation grade, respectively, on the base of the proliferation rate, morphology and on the capacity to synthesize albumin/ferritin, known markers of hepatic differentiation (Grassi et al., 2007b).

After having verified that the aptamer transfection efficiencies were similar among the different cell lines (Supl. mat 2), we evaluated the effects of GT75 on cell viability compared to the control aptamer CT75. In all cell lines, GT75 effect was time dependent (data not shown) reaching its maximum at day ten after transfection in 96-well-plate cultured cells. At this time point, a dose dependent effect was observed in all cell lines (Fig. 2). Interestingly, the less differentiated JHH6 appeared to be the most sensible to GT75 as they displayed a specific sensibility already at the concentration of 125 nM; in contrast, in the more differentiated HuH7 and HepG2, optimal effects were visible at 250 and 500 nM, respectively.

Because of the sensitivity to low GT75 dose, JHH6 were chosen for further testing. The viability data were asseded also by cell counting (Fig. 3) confirming the ability of GT75 to reduce the expansion of this HCC cell type at a relative low dose. To obtain a precise cell counting, this test was performed in six-well-plates cultured cells. The fact that under this condition cells grew faster compared to the cells cultivated in 96 well, explains why GT75 effect was detectable earlier (days 3–6) compared to the viability test performed in 96-well-plate cultured cells.

Interestingly, GT75 effect was independent from the transfection reagent used (lipofectamine) as its administration as naked molecule to 96-well-plate cultured cells, maintained the ability to reduce cell vitality (Fig. 3B). In this case, however, a much higher concentration was required; additionally, the most evident effects were visible earlier (3–6 days from administration) compared to GT75 delivered by liposome in 96-well-plate cultured cells. Finally, in JHH6 we confirmed our previous observation that in cell lines derived from solid tumors, GT27 and GT51 have far less effectiveness compared to GT75 (Supl. mat 3).

### 3.3. Effect of GT75 on cell cycle, apoptosis and necrosis in JHH6 cells

To understand the mechanism(s) ruling GT75 effect on JHH6 vitality, we evaluated the possible interference with the cell cycle in cells cultured in 6 well plate. Compared to controls, no relevant influences on the distribution of the cells in the different phases of the cell cycle were observed both after 3 (Fig. 4A) and 6 (Fig. 4B) days from GT75 administration at 125 nM; similar results were observed at higher GT75 concentration (data not shown). In contrast, a significant induction of apoptosis was observed (Fig. 4C)

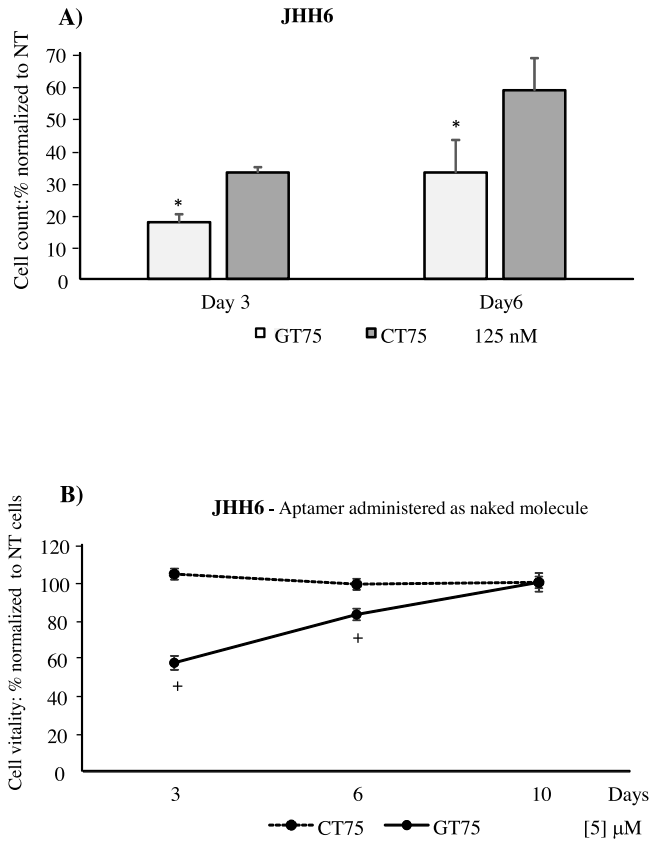


**Fig. 3.** Effects of GT75 in JHH6. (A) Effect on cell number of 125 nM-GT75 delivered by lipofection to six-well-plate cultured JHH6 compared to the control CT75 treated cells. The results are reported as% of non-treated cells (NT); data are expressed as means ± SEM, n = 6. *$p < 0.009$, compared to CT75 treated cell. (B) Effects (MTT) on cell viability of GT75 administered as naked molecule (5 μM) to 96-well-plate cultured JHH6; the results are reported as% of non-treated cells (NT); data are expressed as means ± SEM, n = 6. +$p < 0.028$, compared NT.

3 days after GT75 administration, compared to control. Notably, 6 days after aptamer treatment, apoptosis rate did not differ from control (Fig. 4D) indicating that at this time point the aptamer-induced apoptotic effect was over. Finally, no significant induction of cell necrosis was observed (Fig. 4E).

### *3.4. Effect of GT75 on eEF1A expression levels in JHH6 cells*

The important effect on cell vitality of GT75, prompted us to verify whether this was dependent on any variations in the intracellular levels of the eEF1A isoforms. Our data revealed no significant variation at the mRNA levels both three (Fig. 5A and C) and six days (data not show) following aptamer transfection. At the protein level, only a tendency towards a slight reduction was observed three (Fig. 5B and D) and six days (data not show) following aptamer transfection.

### *3.5. Effect of GT75 conjugated with cholesterol in JHH6*

Disappointingly, the conjugation of GT75 with cholesterol (GT75-chol) did not show any specific effect on JHH6 viability at all the different time points (Fig. 6A) and concentration tested (125–500 nM, data not shown). As CD analysis excluded a cholesterol-induced mis-folding of the aptamer (Fig. 6B), we investigated the uptake properties of GT75-chol conjugating the compound with fluorescein (GT75-chol-FITC). Interestingly, GT75-chol-FITC gave origin to a rather spotted cellular pattern with a certain degree of accumulation in defined cellular regions of the cell (Fig. 7A). Notably, GT75-chol-FITC did not efficiently reach the nucleus, as this cellular compartment was perfectly visible (Fig. 7B, nuclear DAPI staining). We can be sure that GT75-chol-FITC entered the cells as confocal microscopy showed the green FITC signal inside the cell (Fig. 7C and Supl. mat 4). We thus concluded that a possible reason for the lack of GT75-chol activity could be due to the segregation in cellular compartments, which prevented GT75-chol to reach the target protein. To prove this hypothesis we transfected GT75-chol-FITC in the presence of lipofectamine (GT75-chol-FITC/LF) used to transfect GT75. The GT75-chol-FITC/LF gave origin to an even cytoplasmic distribution with nuclear localization (Fig. 7E, I-II-III), substantially resembling the pattern obtained by GT75-FITC/LF (Fig. 7D, I-II-III). Interestingly, the restoration of the proper cellular distribution was paralleled by the reestablishment of GT75-chol activity (Fig. 7F), strongly supporting the concept that the lack of activity was mainly due to the segregation in defined cellular compartments.

### *3.6. GT75 increases the therapeutic index of bortezomib and idarubicin*

The combination of different drugs as a strategy to improve the outcome of HCC patients has drawn wide attention in recent years. Thus, we studied the effect of GT75 administered in combination with the anticancer drugs bortezomib and idarubicin. Two different experimental schemes were used: in the first, the drug was administered to JHH6 before GT75 delivery *via* lipofection (protocol 1), in the second (protocol 2) after. To investigate whether GT75 could increase the therapeutic index of bortezomib and idarubicin, sub-toxic doses of the two anti-neoplastic agents were employed (Fig. 8, grey columns). Moreover, a GT75 concentration of 125 nM was used, as at this aptamer concentration cell vitality is not completely abrogated (see Fig. 2C). This left the possibility to detect any further drug (bortezomib or idarubicin) effects on cell vitality.

The combination drug/GT75 (protocol 1) markedly improved bortezomib/idarubicin effects on cell vitality (Fig. 8A and C) compared to the drug combined with the control CT75. Notably, also drug/GT75 effects were superior to GT75 alone (significant for 10 nM bortezomib and 2,5–5 ng/ml idarubicin). Interestingly, the potentiating effect of the two drugs was maintained also administering first GT75 and then the drugs (Fig. 8B and D, protocol 2), supporting the solidity of the combined effects of drug/aptamer. Notably, the combination GT75/drug was always superior to the effects of the control CT75/drugs. Only in the case of idarubicin administered at 10 ng/ml, this was not the case, thus indicating under this condition the prevalence of a non-specific effect.

## 4. Discussion

The lack of effective therapies, especially for the advanced form of HCC, makes the identification of novel therapeutic approaches extremely urgent. Here we explore the targeting of eEF1A by means of the GT75 aptamer, showing a great therapeutic potential for this molecule.

GT75 derives from a shorter aptamer version (GT27) shown to be effective in reducing the viability of a variety of leukemic cells (Dapas et al., 2003a; Morassutti et al., 1999; Scaggiante et al., 2006a, 2013b, 1998). Here we provide evidences (Fig. 1) that both aptamers GT75 and GT27 can form the expected complexes in the HCC cell lines tested, thus indicating the ability to specifically binding eEF1A. Despite this, in JHH6, the effectiveness of GT75 delivered by lipofectamine was definitively superior to that of GT27 (Suppl mat 3). We can exclude significant differences in the cellular internalization as GT27-FITC and GT75-FITC resulted in comparable cellular uptake (data not shown). As we have not deeply investigated the biochemistry of GT75 and GT27 binding to eEF1A, we cannot complete exclude differences in the binding

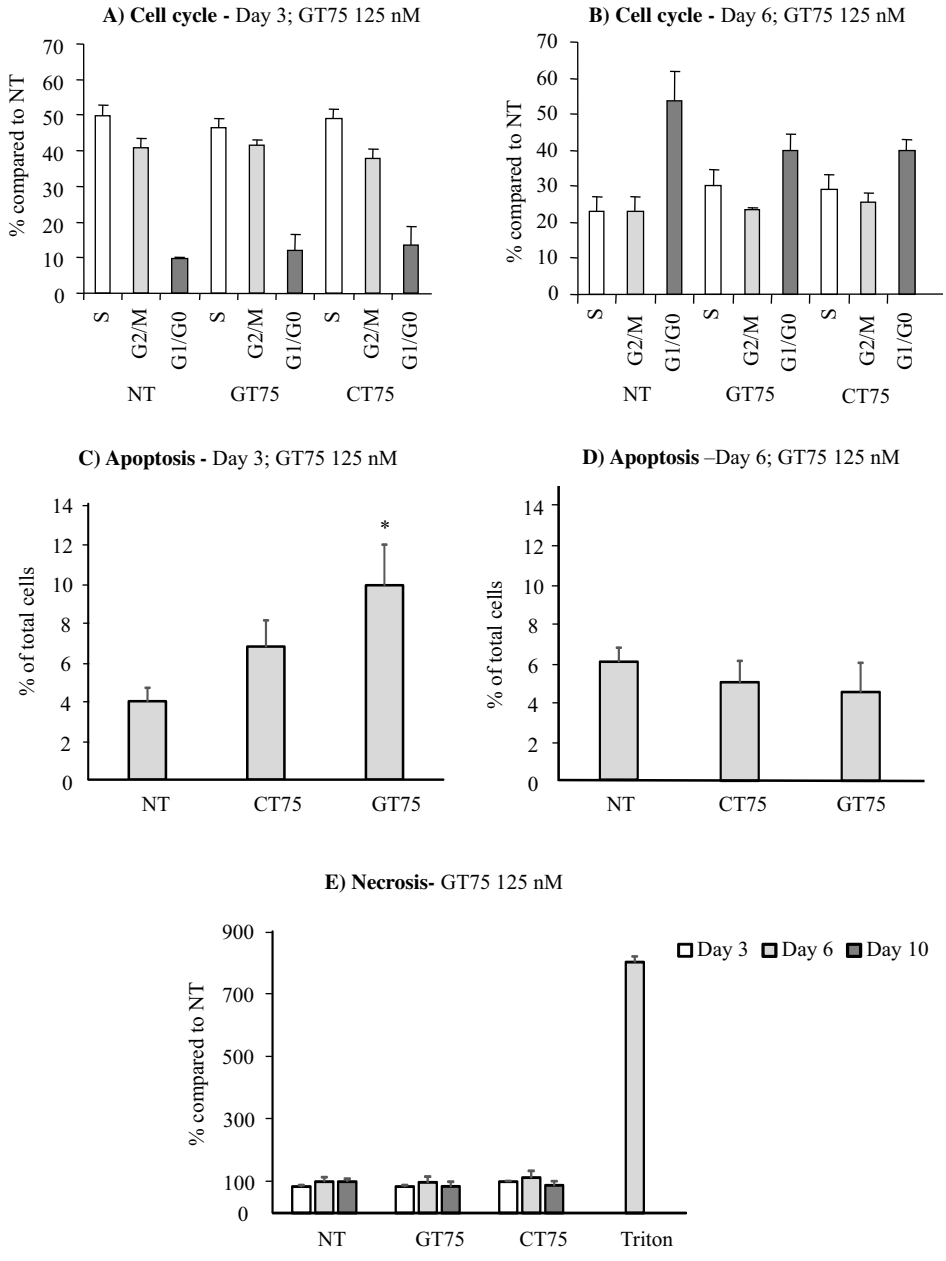


**Fig. 4.** Effects of GT75 on the cell cycle, apoptosis and necrosis induction in JHH6. (A) Cell cycle phase distribution was studied by the double staining DNA procedure 3 (A) and 6 (B) days after lipofection of 125 nM of GT75 to six-well-plate cultured JHH6; the data are reported as the% of total cells; data are expressed as means ± SEM, n = 6. (C) Apoptosis was evaluated by annexin V test 3 and 6 days after GT75 lipofection to six-well-plate cultured JHH6; the results are reported as% of total cells in each treatment; data are expressed as means ± SEM, n = 5. P = 0.008, compared to CT75 treated cells. (D) Cell necrosis induction was evaluated by LDH assay at different time points after GT75 lipofection to 96-well-plate cultured JHH6; triton X-100 (1% of final concentration): positive control; the results are reported as% of non-treated cells (NT); data are expressed as means ± SEM, n = 6.

affinity. It is also possible that, being longer, GT75 has an extended cytoplasmic half-life thus resulting in a prolonged interaction with eEF1A. Cell-dependent mechanisms can also concur to determine the different biological effectiveness as GT27 was very effective in leukemic cells (Dapas et al., 2003a; Morassutti et al., 1999; Scaggiante et al., 2006a, 2013b, 1998) but not in HCC cell lines.

Our data (Fig. 2) indicate that GT75 delivered by lipofectamine can efficiently affect the viability of a panel of HCC cell lines, thus showing its broad potential effectiveness against different HCC phenotypes. Notably, the less differentiated HCC cell line JHH6, appears to be the most sensitive to the aptamer action. We can exclude significant differences in the cellular uptake as GT75-FITC internalization is comparable in all HCC cell lines (Sup mat 2). In contrast, the fact that JHH6 have the highest level of eEF1A1 compared to HuH7 and HepG2 (Grassi et al., 2007a) may indicate that this cell line is more dependent on eEF1A1 canonical and non-canonical functions for its survival. Another reason for the increased JHH6 sensibility to GT75 may depend on the occurrence of post-translational modifications of eEF1A, which promote the affinity to GT75. In this regard, we have observed (Scaggiante et al., 2013b) that the effectiveness of GT27 in the leukemic cell line CCRF-CEM was strictly dependent on the presence of a post-translational modified form of eEF1A.

The involvement of eEF1A in cell proliferation and apoptosis (Ruest et al., 2002; Scaggiante et al., 2012; Talapatra et al., 2002) prompted us to verify whether these biological events could have been affected by the GT75 targeting eEF1A. In JHH6, no relevant influences were observed at the cell cycle level (Fig. 4A and B), a

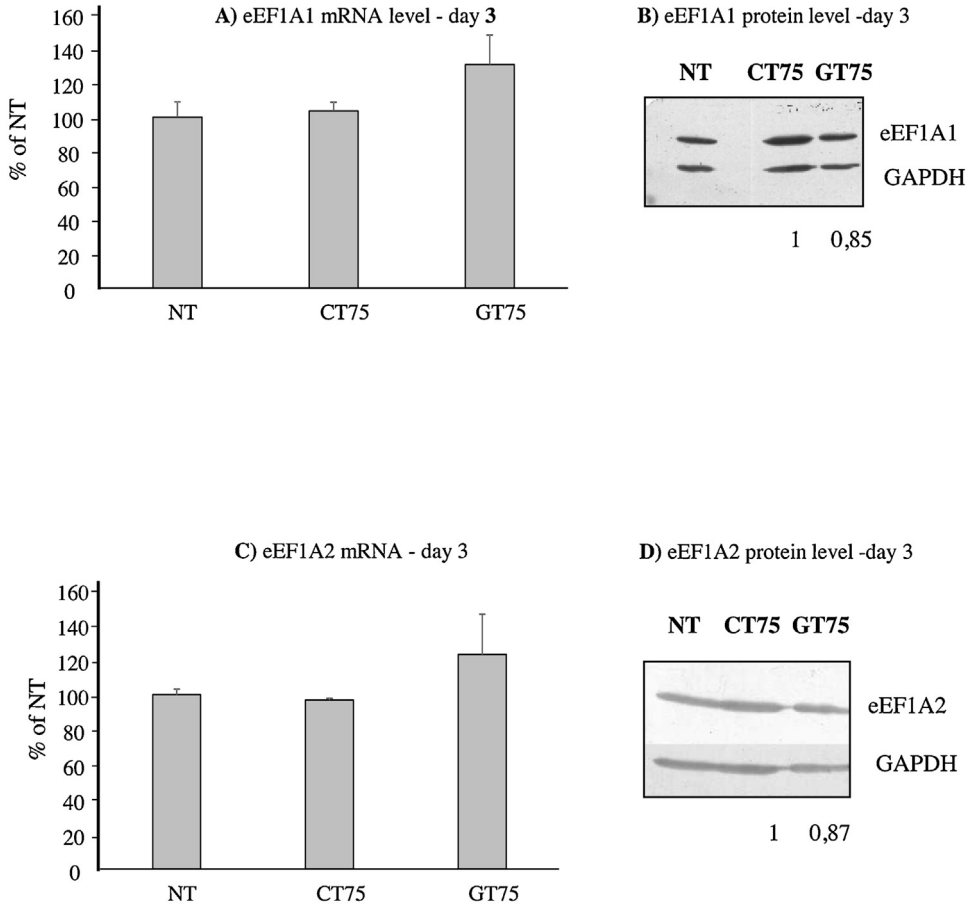


**Fig. 5.** Effects of GT75 on the expression level of eEF1A. (A and C) 125 nM of GT75 were delivered by lipofection to six-well-plate cultured JHH6; the levels of eEF1A1 and eEF1A2 mRNAs were evaluated three days after delivery; the results are reported as% of non-treated cells (NT); data are expressed as means ± SEM, n = 5. (B and D) 125 nM of GT75 were delivered by lipofection to six-well-plate cultured JHH6; the levels of eEF1A1 and eEF1A2 proteins were evaluated three days after delivery (representative western blotting); GAPDH was used as normalizator.

fact that may apparently be in contrast with a previous work by Schlaeger et al. (2008b). In this case, the siRNA mediated silencing of the eEF1A2 isoform, resulted in a clear impairment of HCC cell proliferation. This apparent discrepancy may be explained by the substantial different approach employed to target eEF1A, *i.e* siRNA mediated silencing in Schlaeger et al. (2008b) and aptameric targeting (our work). Whereas the siRNA-based approach represses the synthesis of eEF1A2, thus reducing both the cytoplasmic and the cytoskeletal-nuclear fractions of the protein, our aptameric-based approach mainly interacts with the cytoskeletal/nuclear fraction (Dapas et al., 2003b; Scaggiante et al., 2006b). Additionally, our GT75 may preferentially target the eEF1A1 isoform (see below). It is thus conceivable that targeting different sub cellular fractions of the eEF1A protein and probably different isoforms, the results at the phenotypic levels can be divergent. In spite of the apparent discrepancy at the cell cycle level, the GT75 treatment significantly increased the apoptotic rate (Fig. 4D), in agreement with the work of Schlaeger et al. (2008b). Given the described anti-apoptotic role of eEF1A in different tumor cell type (Chang and Wang, 2007; Ruest et al., 2002; Talapatra et al., 2002), it is reasonable to hypothesize that in JHH6 the impairment of eEF1A functions can destabilize its anti-apoptotic properties. Notably, the extent of apoptosis induction is more contained (Fig. 4C) compared to the reduction of cell viability (Fig. 2). This opens the possibility that other cell death mechanisms may concur to determine the marked reduction in cell viability induced by GT75. Among these, however, our data exclude cell necrosis (Fig. 4E). Future investigation are required (work in progress) better define this aspect and to dissect the molecular pathway(s) responsible for the potent suppression of cell vitality we observed.

The phenotypic effects of GT75 most likely depend on the direct interaction with the eEF1A protein. This is supported by the fact that GT75 treatment neither grossly affects the mRNA (Fig. 5A and C) nor the protein levels (Fig. 5B and D) of the eEF1A isoforms. Thus, it is conceivable that GT75 may impair/prevent eEF1A interactions with other partners. It remains to be clarified whether or not GT75 can bind to both eEF1A isoforms. The GT27 aptamer, from which GT75 has been derived, was able to bind to eEF1A protein (Dapas et al., 2003a; Morassutti et al., 1999; Scaggiante et al., 2006a). Additionally, binding assay we performed (Scaggiante et al., unpublished results) using adult rat muscle cell extract expressing only the eEF1A2 isoform (99% identity with human protein), suggested that GT75 has low affinity for eEF1A2. Further *in vitro* testing are required to better characterize GT75 affinity for eEF1A2.

With the aim to explore in the future the effectiveness of GT75 in *in vivo* HCC models, in this work we investigated the possibility to conjugate our aptamer with cholesterol. Cholesterol has the potentiality to drive the aptamer to hepatic cells that possess cholesterol receptor (Healy et al., 2004; Krutzfeldt et al., 2005; Manoharan, 2002), thus favoring a liver-targeted delivery. This in principle allows the localization of the therapeutic molecule at the desired site minimizing possible side effect due to cell mis-targeting. Despite being effective in promoting cell internalization of GT75 (Fig. 7A–C, Suppl mat 4), cholesterol induced the compartmentalization in discrete vesicles in the

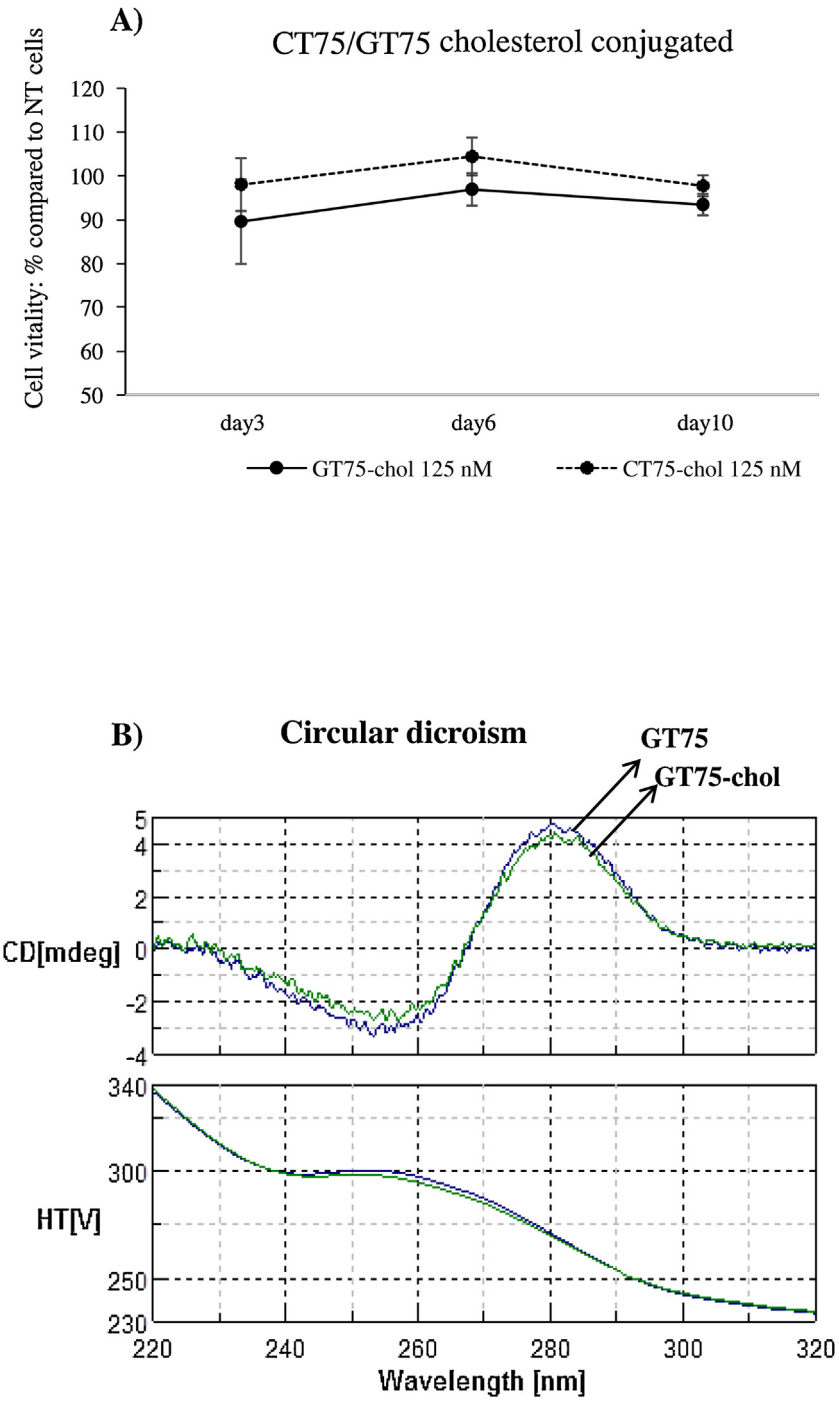


**Fig. 6.** Effects of cholesterol-conjugated GT75 on JHH6 viability. GT75 conjugated with cholesterol (GT75-chol, 125 nM) was administered to 96-well-plate cultured JHH6 at different concentrations (A) with the effects on viability (MTT) being evaluated ten days after administration. The results are reported as% of non-treated cells (NT); data are expressed as means ± SEM, n = 5. (B) Circular dichroism of 0.5 μM GT75 and cholesterol-conjugated GT75 (GT75-chol) in phosphate buffer, pH7.0 at 220–320 nm. Blue = GT75; Green = GT75chol. (For interpretation of the references to colour in this figure legend, the reader is referred to the web version of this article.)

cytoplasm of GT75 with the exclusion of the nucleus. This segregation resulted in a complete abrogation of GT75 activity. Notably, the activity loss is not attributable to a different conformation of the GT75 induced by the presence of the cholesterol molecule. Indeed, the CD analysis did not show differences among positive and negative peaks in GT75 and GT75-cholesterol samples (Fig. 6B). Moreover, the delivery of GT75-Chol by lipofectamine (compare Fig. 7E with D), restored both the proper intracellular distribution and the aptamer activity (Fig. 7F). We believe that the nuclear/cytoskeletal localization is particularly important as eEF1A1 tend to be localized in these cell regions where it is involved, for example, in the nuclear export of heat shock proteins (HSP) (Vera et al., 2014), often upregulated in HCC (Lu et al., 2009; Yang et al., 2015). Moreover, our previous works showed that the shorter GT aptamers, from which the present GT75 is derived, can bind to the eEF1A protein present in the nuclear/cytoskeletal-enriched cell compartment (Dapas et al., 2003a; Morassutti et al., 1999; Scaggiante et al., 2006a, 2013b, 1998) but not that present in the soluble cytosolic compartment. Thus, our data indicate the relevance of the proper subcellular

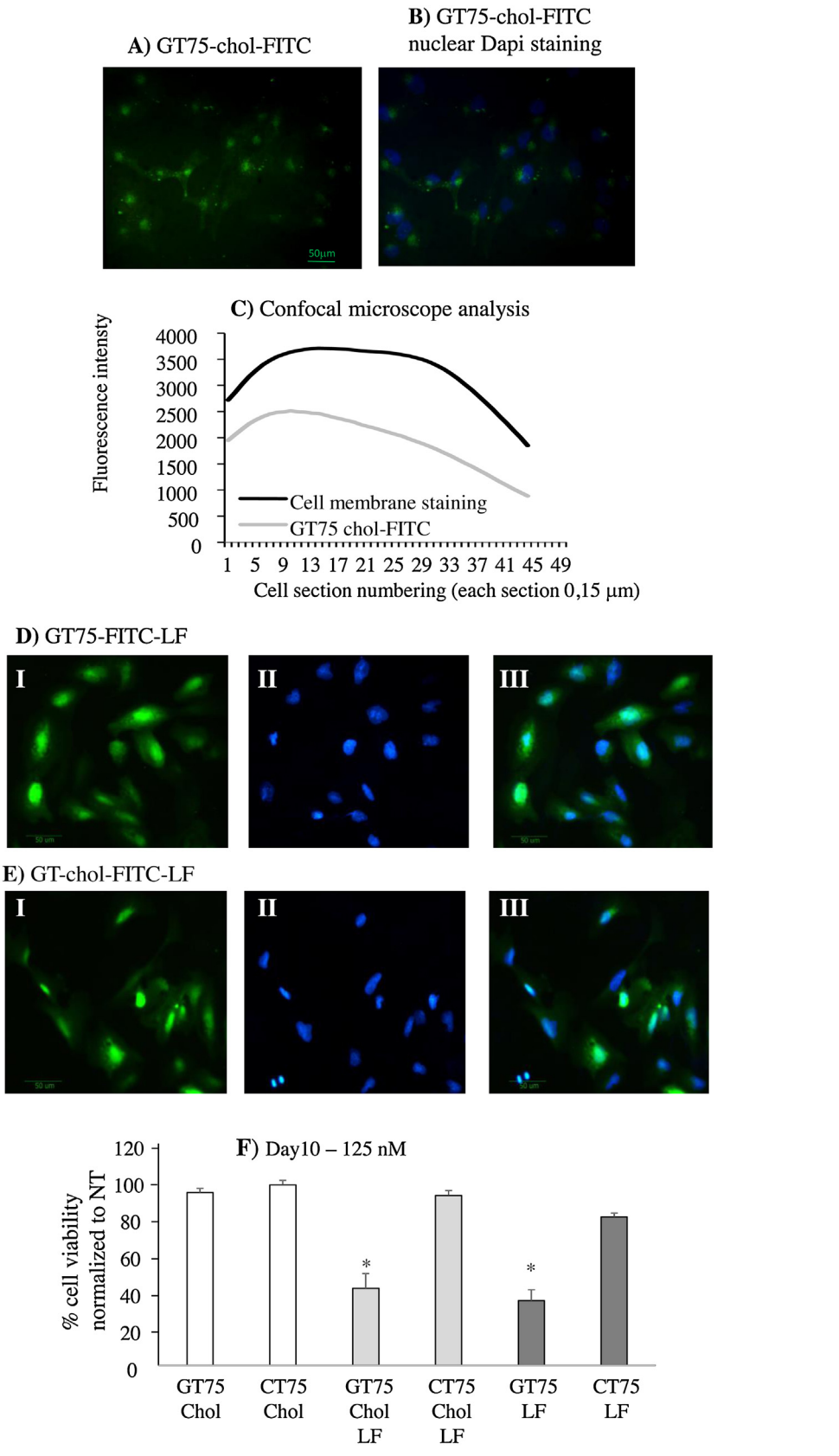


**Fig. 7.** JHH6 uptake of cholesterol-conjugated GT75 and cholesterol-conjugated GT75 delivered by lipofection. (A and B) Cholesterol-conjugated GT75 labelled by fluorescein (GT75-chol-FITC) was delivered at 125 nM to six-well-plate cultured JHH6; 4 h after delivery, cells were fixed and the nucleus stained by DAPI; (C) 4 h after JHH6 transfection by GT75-chol-FITC, cells were collected and stained by the vital dye FastDil™ (red) which stains the cellular membrane and the cytoskeleton. Afterword the red and green fluorescence intensities were measured by confocal microscopy in multiple cell sections. (D and E) Comparison of cell distribution for GT75-FITC-LF (D) and GT75-chol-FITC-LF (E) in fixed JHH6 4 h after transfection; I, II and III corresponds to section stained in green (aptamer-FITC), in blue (DAPI) and the overlay, respectively. LF: lipofectamine. (F) Effects on cell vitality of GT75/CT75 with and without conjugation with cholesterol (chol) and delivered in the presence or absence of the LF (day 10 after transfection, [125 nM]). (For interpretation of the references to colour in this figure legend, the reader is referred to the web version of this article.)

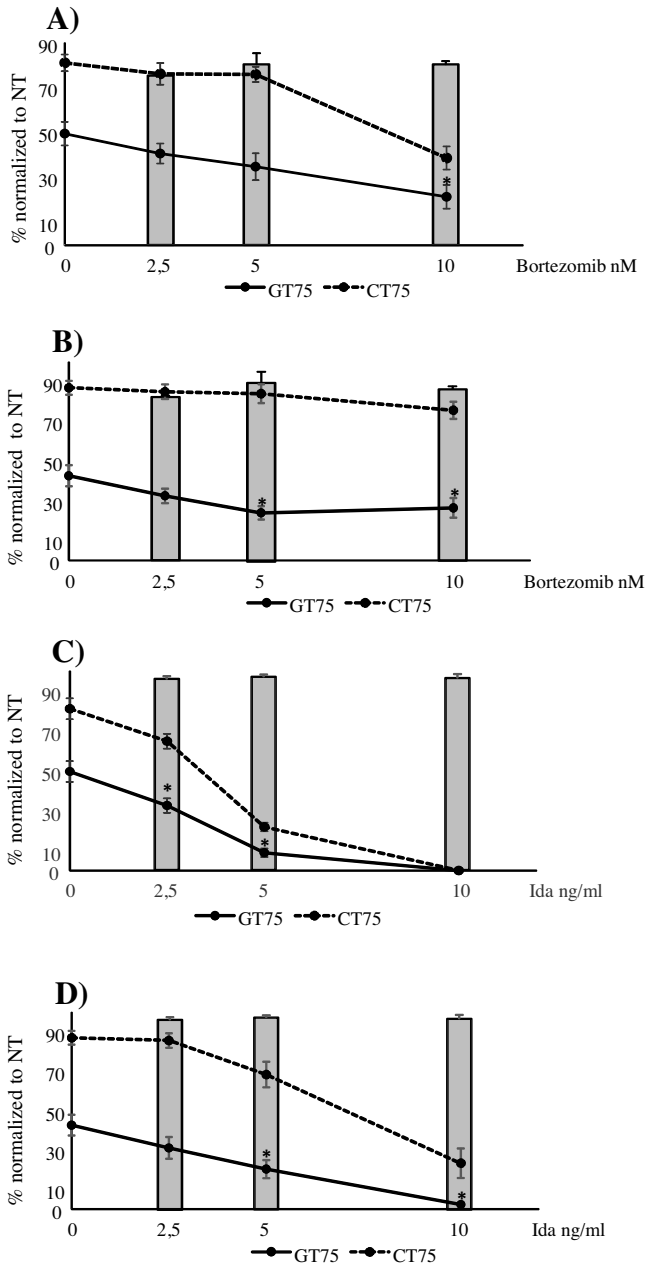


**Fig. 8.** Improvement of the therapeutic index of bortezomib and idarubicin by GT75. 96-well-plate cultured JHH6 were either (A) treated by bortezomib first and then lipofected by 125 nM GT75 or (B) *vice versa*; cell viability was measured by MTT ten days after the beginning of the treatment. The grey columns indicate the treatment by bortezomib alone. The results are reported as% of non-treated cells (NT); data are expressed as means ± SEM, n = 6. *$p < 0.03$, compared to bortezomib-treated JHH6 and GT75-treated JHH6. (C and D) as in A and B except that idarubicin was used.

localization for our aptamer to be biologically effective. This observation is in line with the knowledge that aptamers and more in general of nucleic acid based drugs (Grassi et al., 2005, 2010; Scaggiante et al., 2011), need to reach the appropriate cellular compartment for optimal activity. Moreover, our observation suggests caution with regard to the use of cholesterol-bound aptamers, despite the reported advantages of this delivery approach for the liver.

The highly heterogeneous nature of HCC, mostly dependent on the activation of multiple cancer promoting genes (Cabibbo et al., 2012), suggests that the targeting of multiple tumorigenic molecules can result in a more effective control of HCC expansion. Our data (Fig. 8) indicate that liposome-delivered GT75 can remarkably increase the therapeutic index of bortezomib and of idarubicin. Notably, the effect is independent from the administration protocol, *i.e* first the drug and then GT75 or *vice versa*. This demonstrates the robustness of the therapeutic interaction observed. Moreover, the fact that GT75 can improve the therapeutic index of drugs with completely different mechanism of action (proteasome inhibitor, bortezomib and topoisomerase I inhibitor, idarubicin), demonstrates its pleiotropic ability to synergize with conventional antineoplastic drugs, similarly to what observed for GT27 (Dapas et al., 2002). Thus, our findings indicate GT75 as a molecule with the potential to be effectively used in combination with conventional anticancer drugs in the treatment of HCC.

Although not at the same extent of GT75/lipofectamine, also CT75/lipofectamine seems to potentiate the effects of bortezomib and idarubicine. Given that CT75 cannot bind eEF1A (see Fig. 1C), we believe this mostly depends on a non-specific toxicity exerted by lipofectamine. Indeed lipofectamine *per se* has a detrimental effect on cell vitality (see Fig. 2C, 125 nM). Moreover, CT75 administered in the naked form has negligible effects on cell vitality (Fig. 3B). Thus, it is convincible that in the CT75/lipofectamine complex, the effect of lipofectamine combines with the effects of the two drugs resulting in a non-specific potentiation of drug action.

In conclusion, the lipofectamine-mediated but not the cholesterol-mediated delivery of GT75 was effective in delivering GT75, resulting in the impairment of the viability of HCC derived cells. Additionally, the lipofectamine-mediated delivery of GT75 markedly improved the therapeutic index of the anticancer drugs bortezomib and idarubicin. Together our findings strongly support the great therapeutic potential of GT75.

## Acknowledgements

This work was in part supported by the "Fondazione Cassa di Risparmio of Trieste", by the "Fondazione Benefica Kathleen Foreman Casali of Trieste", by the "Beneficentia Stiftung" of Vaduz Liechtenstein, by the Italian Minister of Instruction, University and Research (MIUR), PRIN 2010-11, [20109PLMH2] and by "5 per mille 2013" of Lega Italiana per la Lotta contro i Tumori (LILT), Italian Minister of Health.

## References

Abbas, W., Kumar, A., Herbein, G., 2015. The eEF1A proteins: at the crossroads of oncogenesis, apoptosis, and viral infections. Front. Oncol. 5, 75.
Azmi, A.N., Chan, W.K., Goh, K.L., 2015. Sustained complete remission of advanced hepatocellular carcinoma with sorafenib therapy. J. Dig. Dis. 16 (9), 537–540.
Baiz, D., Pozzato, G., Dapas, B., Farra, R., Scaggiante, B., Grassi, M., Uxa, L., Giansante, C., Zennaro, C., Guarnieri, G., Grassi, G., 2009. Bortezomib arrests the proliferation of hepatocellular carcinoma cells HepG2 and JHH6 by differentially affecting E2F1, p21 and p27 levels. Biochimie 91, 373–382.
Baiz, D., Dapas, B., Farra, R., Scaggiante, B., Pozzato, G., Zanconati, F., Fiotti, N., Consoloni, L., Chiaretti, S., Grassi, G., 2014. Bortezomib effect on E2F and cyclin family members in human hepatocellular carcinoma cell lines. World J. Gastroenterol. 20, 795–803.
Barba, A.A., Lamberti, G., Sardo, C., Dapas, B., Abrami, M., Grassi, M., Farra, R., Tonon, F., Forte, G., Musiani, F., Licciardi, M., Pozzato, G., Zanconati, F., Scaggiante, B., Grassi, G., Cavallaro, G., 2015. Novel lipid and polymeric materials as delivery systems for nucleic acid based drugs. Curr. Drug Metab. 16, 427–452.
Bochicchio, Dalmoro, S.A., Barba, A.A., Grassi, G., Lamberti, G., 2015. Liposomes as siRNA delivery vectors. Curr. Drug Metab. 15 (9), 882–892.

Burnett, J.C., Rossi, J.J., Tiemann, K., 2011. Current progress of siRNA/shRNA therapeutics in clinical trials. Biotechnol. J. 6, 1130–1146.
Cabibbo, G., Maida, M., Genco, C., Parisi, P., Peralta, M., Antonucci, M., Brancatelli, G., Camma, C., Craxi, A., Di Marco, V., 2012. Natural history of untreatable hepatocellular carcinoma: a retrospective cohort study. World J. Hepatol. 4, 256–261.
Chang, R., Wang, E., 2007. Mouse translation elongation factor eEF1A-2 interacts with Prdx-I to protect cells against apoptotic death induced by oxidative stress. J. Cell. Biochem. 100, 267–278.
Chen, Y.J., Wu, H., Shen, X.Z., 2015. The ubiquitin-proteasome system and its potential application in hepatocellular carcinoma therapy. Cancer Lett. S0304-3835(15)00442-5.
Dapas, B., Perissin, L., Pucillo, C., Quadrifoglio, F., Scaggiante, B., 2002. Increase in therapeutic index of doxorubicin and vinblastine by aptameric oligonucleotide in human T lymphoblastic drug-sensitive and multidrug-resistant cells. Antisense Nucleic Acid Drug Dev. 12, 247–255.
Dapas, B., Tell, G., Scaloni, A., Pines, A., Ferrara, L., Quadrifoglio, F., Scaggiante, B., 2003a. Identification of different isoforms of eEF1A in the nuclear fraction of human T-lymphoblastic cancer cell line specifically binding to aptameric cytotoxic GT oligomers. Eur. J. Biochem. 270, 3251–3262.
Dapas, B., Tell, G., Scaloni, A., Pines, A., Ferrara, L., Quadrifoglio, F., Scaggiante, B., 2003b. Identification of different isoforms of eEF1A in the nuclear fraction of human T-lymphoblastic cancer cell line specifically binding to aptameric cytotoxic GT oligomers. Eur. J. Biochem. 270, 3251–3262.
Dapas, B., Farra, R., Grassi, M., Giansante, C., Fiotti, N., Uxa, L., Rainaldi, G., Mercatanti, A., Colombatti, A., Spessotto, P., Lacovich, V., Guarnieri, G., Grassi, G., 2009. Role of E2F1-cyclin E1-cyclin E2 circuit in human coronary smooth muscle cell proliferation and therapeutic potential of its downregulation by siRNAs. Mol. Med. 15, 297–306.
Di Costanzo, G.G., Tortora, R., 2015. Intermediate hepatocellular carcinoma: how to choose the best treatment modality? World J. Hepatol. 7, 1184–1191.
Farra, R., Dapas, B., Pozzato, G., Giansante, C., Heidenreich, O., Uxa, L., Zennaro, C., Guarnieri, G., Grassi, G., 2010. Serum response factor depletion affects the proliferation of the hepatocellular carcinoma cells HepG2 and JHH6. Biochimie 92, 455–463.
Farra, R., Dapas, B., Pozzato, G., Scaggiante, B., Agostini, F., Zennaro, C., Grassi, M., Rosso, N., Giansante, C., Fiotti, N., Grassi, G., 2011. Effects of E2F1-cyclin E1-E2 circuit down regulation in hepatocellular carcinoma cells. Dig. Liver Dis. 43, 1006–1014.
Favelier, S., Boulin, M., Hamza, S., Cercueil, J.P., Cherblanc, V., Lepage, C., Hillon, P., Chauffert, B., Krause, D., Guiu, B., 2013. Lipiodol trans-arterial chemoembolization of hepatocellular carcinoma with idarubicin: first experience. Cardiovasc. Interv. Radiol. 36, 1039–1046.
Ferlay, J., Soerjomataram, I., Dikshit, R., Eser, S., Mathers, C., Rebelo, M., Parkin, D.M., Forman, D., Bray, F., 2015. Cancer incidence and mortality worldwide: sources, methods and major patterns in GLOBOCAN 2012. Int. J. Cancer 136, E359–E386.
Grassi, G., Schneider, A., Engel, S., Racchi, G., Kandolf, R., Kuhn, A., 2005. Hammerhead ribozymes targeted against cyclin E and E2F1 cooperate to down-regulate coronary smooth muscle cell proliferation. J. Gene Med. 7, 1223–1234.
Grassi, G., Scaggiante, B., Farra, R., Dapas, B., Agostini, F., Baiz, D., Rosso, N., Tiribelli, C., 2007a. The expression levels of the translational factors eEF1A 1/2 correlate with cell growth but not apoptosis in hepatocellular carcinoma cell lines with different differentiation grade. Biochimie 89, 1544–1552.
Grassi, G., Scaggiante, B., Farra, R., Dapas, B., Agostini, F., Baiz, D., Rosso, N., Tiribelli, C., 2007b. The expression levels of the translational factors eEF1A 1/2 correlate with cell growth but not apoptosis in hepatocellular carcinoma cell lines with different differentiation grade. Biochimie 89, 1544–1552.
Grassi, M., Cavallaro, G., Scirè, S., Scaggiante, B., Daps, B., Farra, R., Baiz, D., Giansante, C., Guarnieri, G., Perin, D., Grassi, G., 2010. Current strategies to improve the efficacy and the delivery of nucleic acid based drugs. Curr. Signal Transduct. Ther. 5, 92–120.
Grassi, G., Scaggiante, B., Dapas, B., Farra, R., Tonon, F., Lamberti, G., Barba, A., Fiorentino, S., Fiotti, N., Zanconati, F., Abrami, M., Grassi, M., 2013. Therapeutic potential of nucleic acid-based drugs in coronary hyper-proliferative vascular diseases. Curr. Med. Chem. 20, 3515–3538.
Healy, J.M., Lewis, S.D., Kurz, M., Boomer, R.M., Thompson, K.M., Wilson, C., McCauley, T.G., 2004. Pharmacokinetics and biodistribution of novel aptamer compositions. Pharm. Res. 21, 2234–2246.
Jemal, A., Bray, F., Center, M.M., Ferlay, J., Ward, E., Forman, D., 2011. Global cancer statistics. CA Cancer J. Clin. 61, 69–90.
Kanasty, R., Dorkin, J.R., Vegas, A., Anderson, D., 2013. Delivery materials for siRNA therapeutics. Nat. Mater. 12, 967–977.
Krutzfeldt, J., Rajewsky, N., Braich, R., Rajeev, K.G., Tuschl, T., Manoharan, M., Stoffel, M., 2005. Silencing of microRNAs in vivo with 'antagomirs'. Nature 438, 685–689.
Lamberti, A., Caraglia, M., Longo, O., Marra, M., Abbruzzese, A., Arcari, P., 2004. The translation elongation factor 1A in tumorigenesis: signal transduction and apoptosis: review article. Amino Acids 26, 443–448.
Li, W., Szoka Jr., F.C., 2007. Lipid-based nanoparticles for nucleic acid delivery. Pharm. Res. 24, 438–449.
Lu, W.J., Lee, N.P., Fatima, S., Luk, J.M., 2009. Heat shock proteins in cancer: signaling pathways, tumor markers and molecular targets in liver malignancy. Protein Pept. Lett. 16, 508–516.
Manoharan, M., 2002. Oligonucleotide conjugates as potential antisense drugs with improved uptake biodistribution, targeted delivery, and mechanism of action. Antisense Nucleic Acid Drug Dev. 12, 103–128.
Mickleburgh, I., Chabanon, H., Nury, D., Fan, K., Burtle, B., Chrzanowska-Lightowlers, Z., Hesketh, J., 2006. Elongation factor 1alpha binds to the region of the metallothionein-1 mRNA implicated in perinuclear localization—importance of an internal stem-loop. RNA 12, 1397–1407.
Morassutti, C., Dapas, B., Scaggiante, B., Paroni, G., Xodo, L., Quadrifoglio, F., 1999. Effect of oligomer length and base substitutions on the cytotoxic activity and specific nuclear protein recognition of GTn oligonucleotides in the human leukemic CCRF-CEM cell line. Nucleosides Nucleotides 18, 1711–1716.
Oh, Y.K., Park, T.G., 2009. siRNA delivery systems for cancer treatment. Adv. Drug Deliv. Rev. 61, 850–862.
Piscaglia, F., Bolondi, L., 2010. The intermediate hepatocellular carcinoma stage: should treatment be expanded? Dig. Liver Dis. 42 (Suppl. 3), S258–S263.
Ruest, L.B., Marcotte, R., Wang, E., 2002. Peptide elongation factor eEF1A-2/S1 expression in cultured differentiated myotubes and its protective effect against caspase-3-mediated apoptosis. J. Biol. Chem. 277, 5418–5425.
Scaggiante, B., Morassutti, C., Dapas, B., Tolazzi, G., Ustulin, F., Quadrifoglio, F., 1998. Human cancer cell lines growth inhibition by GTn oligodeoxyribonucleotides recognizing single-stranded DNA-binding proteins. Eur. J. Biochem. 252, 207–215.
Scaggiante, B., Dapas, B., Perissin, L., Manzini, G., 2005. Aptameric GT oligomers need to be complexed to ethoxylated polyethylenimine as pre-paired duplexes to efficiently exert their cytotoxic activity in human lymphoblastic cancer cells. Biochimie 87, 713–723.
Scaggiante, B., Dapas, B., Grassi, G., Manzini, G., 2006a. Interaction of G-rich GT oligonucleotides with nuclear-associated eEF1A is correlated with their antiproliferative effect in haematopoietic human cancer cell lines. FEBS J. 273, 1350–1361.
Scaggiante, B., Dapas, B., Grassi, G., Manzini, G., 2006b. Interaction of G-rich GT oligonucleotides with nuclear-associated eEF1A is correlated with their antiproliferative effect in haematopoietic human cancer cell lines. FEBS J. 273, 1350–1361.
Scaggiante, B., Dapas, B., Farra, R., Grassi, M., Pozzato, G., Giansante, C., Fiotti, N., Grassi, G., 2011. Improving siRNA bio-distribution and minimizing side effects. Curr. Drug Metab. 12, 11–23.
Scaggiante, B., Dapas, B., Bonin, S., Grassi, M., Zennaro, C., Farra, R., Cristiano, L., Siracusano, S., Zanconati, F., Giansante, C., Grassi, G., 2012. Dissecting the expression of EEF1A1/2 genes in human prostate cancer cells: the potential of EEF1A2 as a hallmark for prostate transformation and progression. Br. J Cancer 106, 166–173.
Scaggiante, B., Dapas, B., Farra, R., Grassi, M., Pozzato, G., Giansante, C., Fiotti, N., Tamai, E., Tonon, F., Grassi, G., 2013a. Aptamers as targeting delivery devices or anti-cancer drugs for fighting tumors. Curr. Drug Metab. 14, 565–582.
Scaggiante, B., Dapas, B., Pozzato, G., Grassi, G., 2013b. The more basic isoform of eEF1A relates to tumour cell phenotype and is modulated by hyper-proliferative/differentiating stimuli in normal lymphocytes and CCRF-CEM T-lymphoblasts. Hematol. Oncol. 31, 110–116.
Scaggiante, B., Dapas, B., Farra, R., Tonon, F., Abrami, M., Grassi, M., Musiani, F., Zanconati, F., Pozzato, G., Grassi, G., 2014a. In: Parsyan, A. (Ed.), Translation Elongation. Springer, pp. 241–265.
Scaggiante, B., Kazemi, M., Pozzato, G., Dapas, B., Farra, R., Grassi, M., Zanconati, F., Grassi, G., 2014b. Novel hepatocellular carcinoma molecules with prognostic and therapeutic potentials. World J. Gastroenterol. 20, 1268–1288.
Schlaeger, C., Longerich, T., Schiller, C., Bewerunge, P., Mehrabi, A., Toedt, G., Kleeff, J., Ehemann, V., Eils, R., Lichter, P., Schirmacher, P., Radlwimmer, B., 2008a. Etiology-dependent molecular mechanisms in human hepatocarcinogenesis. Hepatology 47, 511–520.
Schlaeger, C., Longerich, T., Schiller, C., Bewerunge, P., Mehrabi, A., Toedt, G., Kleeff, J., Ehemann, V., Eils, R., Lichter, P., Schirmacher, P., Radlwimmer, B., 2008b. Etiology-dependent molecular mechanisms in human hepatocarcinogenesis. Hepatology 47, 511–520.
Talapatra, S., Wagner, J.D., Thompson, C.B., 2002. Elongation factor-1 alpha is a selective regulator of growth factor withdrawal and ER stress-induced apoptosis. Cell Death Differ. 9, 856–861.
Vera, M., Pani, B., Griffiths, L.A., Muchardt, C., Abbott, C.M., Singer, R.H., Nudler, E., 2014. The translation elongation factor eEF1A1 couples transcription to translation during heat shock response. Elife 3, e03164.
Whitehead, K.A., Langer, R., Anderson, D.G., 2009. Knocking down barriers: advances in siRNA delivery. Nat. Rev. Drug Discov. 8, 129–138.
Wu, S.Y., McMillan, N.A., 2009. Lipidic systems for in vivo siRNA delivery. AAPS J. 11, 639–652.
Yan, G., You, B., Chen, S.P., Liao, J.K., Sun, J., 2008. Tumor necrosis factor-alpha downregulates endothelial nitric oxide synthase mRNA stability via translation elongation factor 1-alpha 1. Circ. Res. 103, 591–597.
Yang, Z., Zhuang, L., Szatmary, P., Wen, L., Sun, H., Lu, Y., Xu, Q., Chen, X., 2015. Upregulation of heat shock proteins (HSPA12A, HSP90B1, HSPA4, HSPA5 and HSPA6) in tumour tissues is associated with poor outcomes from HBV-related early-stage hepatocellular carcinoma. Int. J. Med. Sci. 12, 256–263.
Yin, H., Kanasty, R.L., Eltoukhy, A.A., Vegas, A.J., Dorkin, J.R., Anderson, D.G., 2014. Non-viral vectors for gene-based therapy. Nat. Rev. Genet. 15, 541–555.
Zhou, J., Shum, K.T., Burnett, J.C., Rossi, J.J., 2013. Nanoparticle-based delivery of RNAi therapeutics: progress and challenges. Pharmaceuticals (Basel) 6, 85–107.